Electronic Supplementary Material (ESI) for Journal of Materials Chemistry A.

Electronic Supplementary Information

Characterizations

Scanning electron microscopy (SEM) images were performed on a ZEISS SUPRA 55. The morphology and structural features of the synthesized samples were further analyzed by transmission electron microscopy (TEM) on a JEM-2010 microscope as well as high-angle annular dark-field scanning transmission electron microscopy (HAADF-STEM). X-ray powder diffraction (XRD) patterns were obtained in PANalytical X'Pert PRO with Cu Kα radiation at $\lambda = 0.154056$ nm. X-ray photoelectron spectroscopy (XPS) measurements were carried out on an ESCALAB MK II spectrometer using Al Kα X-ray radiation excitation. Raman spectroscopic characterization was performed on a Labram HR UV800. Atomic ratios were calculated by using an inductively coupled plasma emission spectrometer (ICAP PRO). Nuclear magnetic resonance (NMR) was performed on an Avance III HD 500 (Bruker). Inductively coupled plasma emission spectroscopy (ICP-OES) was performed on a Thermo Fisher iCAP PRO.

Calculations of FEs for H_2 and formate

As for HER-MOR co-electrolysis system. FE of the electrocatalytic production of H_2 by HER is determined by the drainage method, and FE of MOR conversion to formate was tested using ^{1}H NMR spectroscopy. Here is the equation[1, 2]:

$$\mathrm{FE}\ (\mathrm{H_2}) = (N_{\mathrm{H2\ production}} \times Z_1 \times F)\ /Q_{\mathrm{tot1}} \qquad (1)$$

$$\mathrm{FE}\ (\mathrm{formate}) = (N_{\mathrm{formate\ yield}} \times Z_2 \times F)\ /Q_{\mathrm{tot2}} \qquad (2)$$

Where Q_{tot1} is the total charge passing through the electrode during HER, and Q_{tot2} is the total charge passing through the electrode during MOR, N is the number of moles of H_2 or formate generated,

Z_1=2 and Z_2=4 are the transfer of one mole H_2 and one mole formate, respectively, F=96,485 C mol^{-1} is Faraday's constant.

Theoretical calculations

All the DFT calculations are performed by the Vienna Ab initio Simulation Package (VASP)[3] with the projector augmented wave (PAW) method. [4] The generalized gradient approximation (GGA) for the Perdew Burke-Ernzerhof (PBE)[5] generalized function is used to process the exchange generalized function. To ensure the accuracy of the calculation results the plane wave basis expansion cutoff energy is set to 400 eV. The convergence criterion is 0.05 eV/Å. The Gaussian smearing method (width of 0.2 eV) is used to optimize the partial occupation of the Kohn - Sham (KS) orbitals. The p (4×4) Ni (111) surface was built with 4 layers, where 3 Ni was replaced by Gd to form NiGd (111) surface. The plane structure of graphene with Pyrrole nitrogen was established, loading on the top of metal surfaces. The Brillouin zone was sampled with a Monkhorst grid. A convergence energy threshold of 10^{-4} eV was applied for the self-consistent calculations. The reaction free energy for elementary steps in OER is obtained by the computational hydrogen electrode (CHE) approximation.[6] The adsorption energy is calculated according to the following equation:

$$E_{ad} = E_{surf+adsorbate} - E_{surf} - E_{adsorbate\text{-}ref} \qquad (3)$$

where the surface with adsorbate is denoted by $E_{surf+adsorbate}$, the bare surface is denoted by E_{surf}, and the reference energy of the adsorbate is denoted by $E_{adsorbat\text{-}ref}$. The correction equation for the free energy is as follows (298 K):

$$\Delta G = \Delta E + \Delta G_{ZPE} + \Delta G_U - T\Delta S \qquad (4)$$

where ΔE is the energy change, ΔG_{ZPE} is the correction for zero-point energy, ΔG_U is the correction from inner energy, and ΔS the correction from entropy.[7]

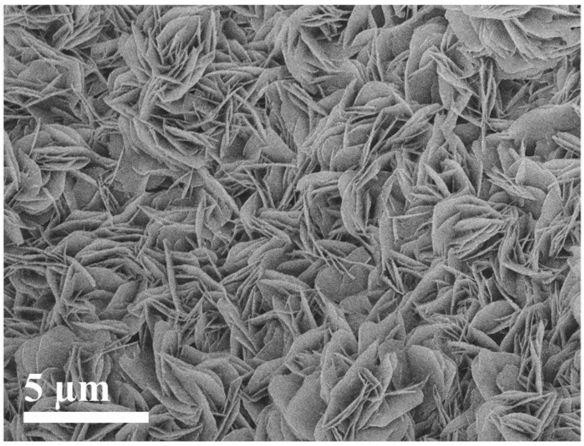

Fig. S1 SEM image of the NiGd-MOF/NF.

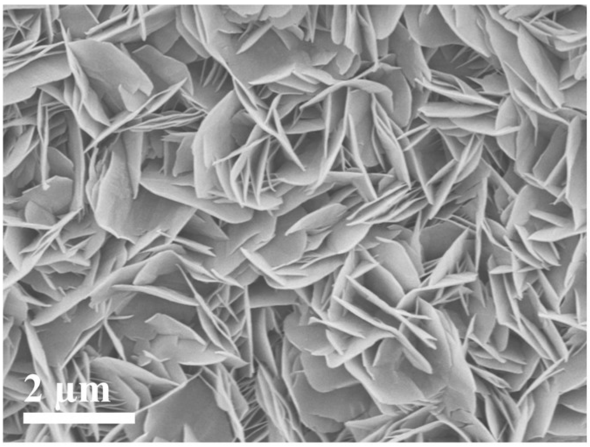

Fig. S2 SEM image of the Ni-MOF/NF.

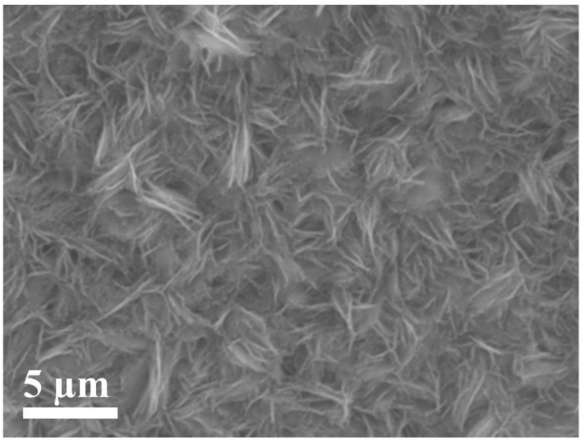

Fig. S3 SEM image of the Ni@N-C/NF.

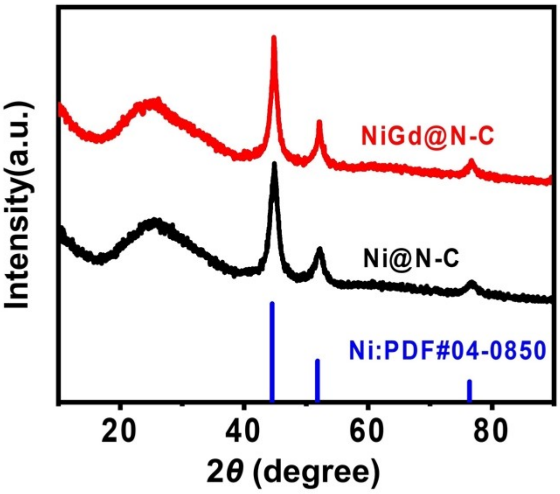

Fig. S4 XRD patterns of NiGd@N-C and Ni@N-C composite nanosheets.

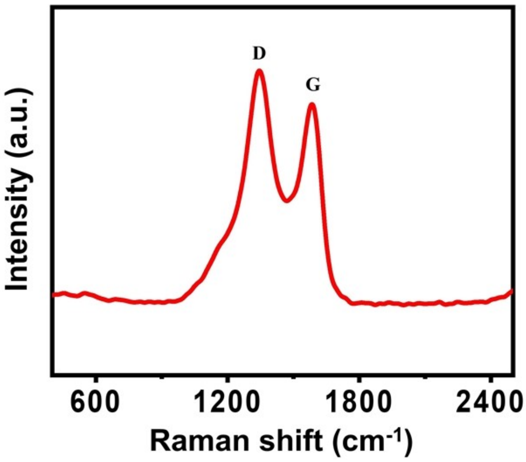

Fig. S5 Raman spectrum of NiGd@N-C composite nanosheets.

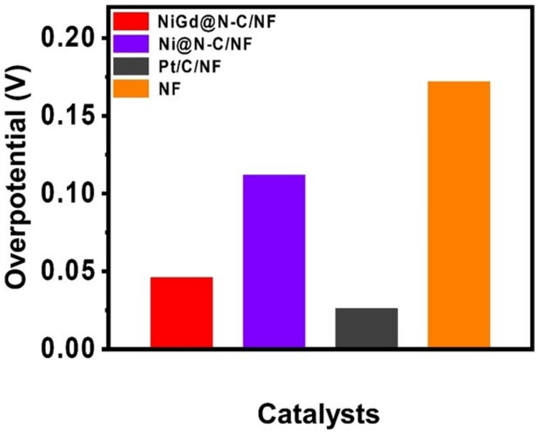

Fig. S6 The require overpotentials for various catalysts at a cathodic current density of 10 mA cm^{-2}.

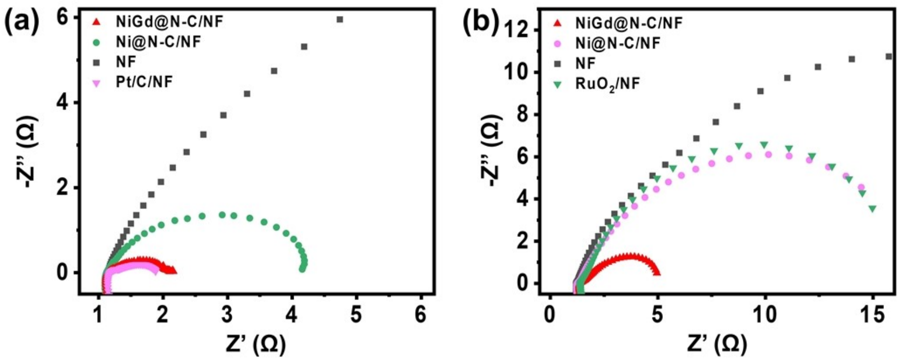

Fig. S7 EIS results of various catalysts in 1.0 M KOH with and without 3.0 M methanol under different applied potentials: (a) -0.05 V (vs. RHE), (b) 1.4 V (vs. RHE).

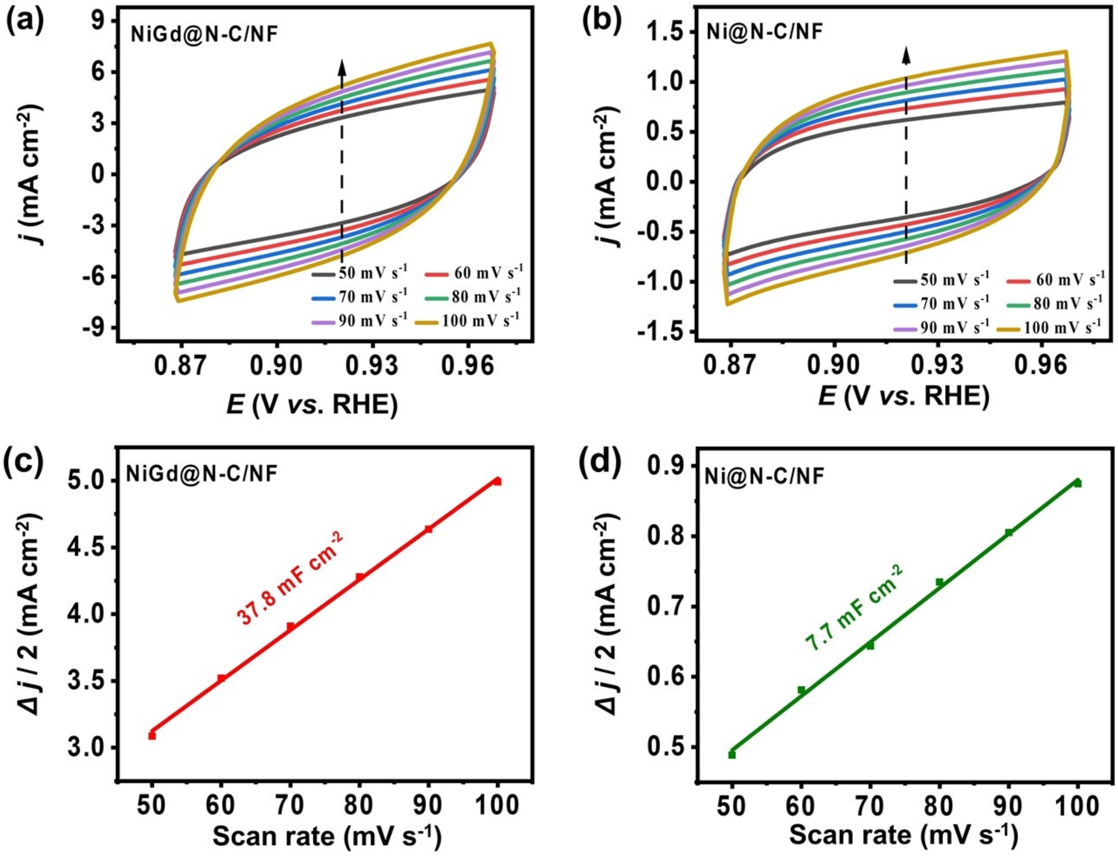

Fig. S8 Electrochemical C_{dl} measurements of (a) NiGd@N-C/NF and (b) Ni@N-C/NF at scan rates of 50, 60, 70, 80, 90 and 100 mV s^{-1}. Capacitance current density versus scan rate for (c) NiGd@N-C/NF and (d) Ni@N-C/NF at 0.92 V (vs. RHE).

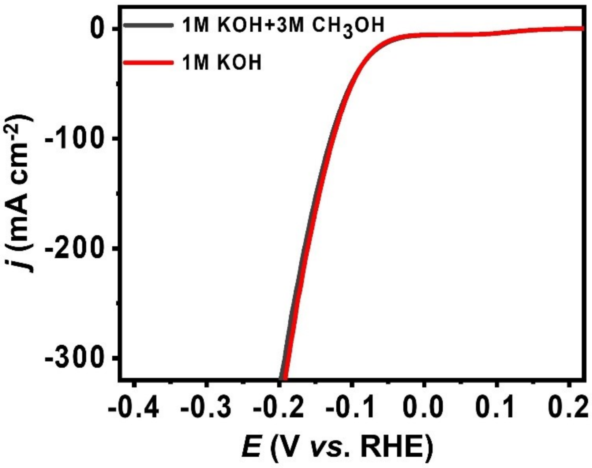

Fig. S9 HER polarization curves of NiGd@N-C/NF in 1.0 M KOH solution in the presence or absence of 3 M methanol.

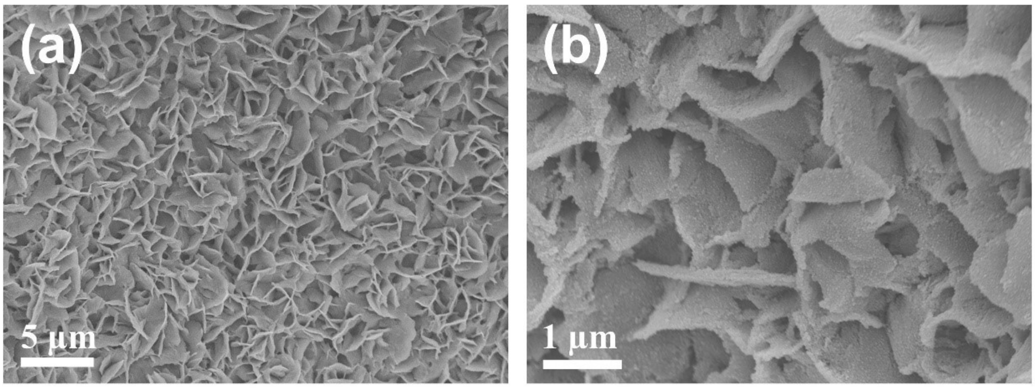

Fig. S10 SEM images of the post-HER NiGd@N-C/NF.

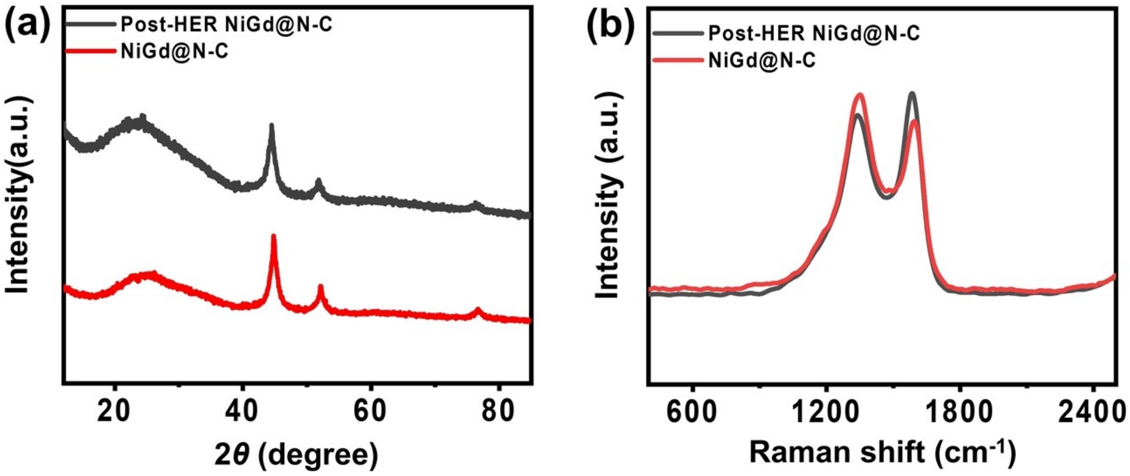

Fig. S11. XRD patterns and Raman spectra of the initial and post-HER NiGd@N-C.

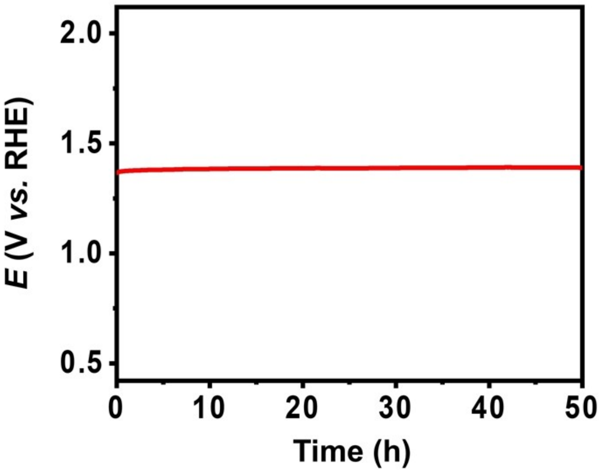

Fig. S12 V-t curve of NiGd@N-C/NF with constant current of 10 mA cm^{-2} for 50 h (without iR correction).

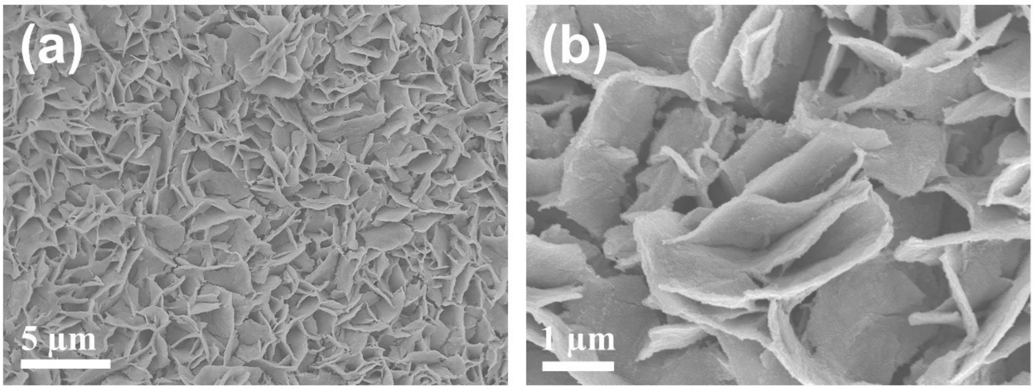

Fig. S13 SEM images of the post-MOR NiGd@N-C/NF.

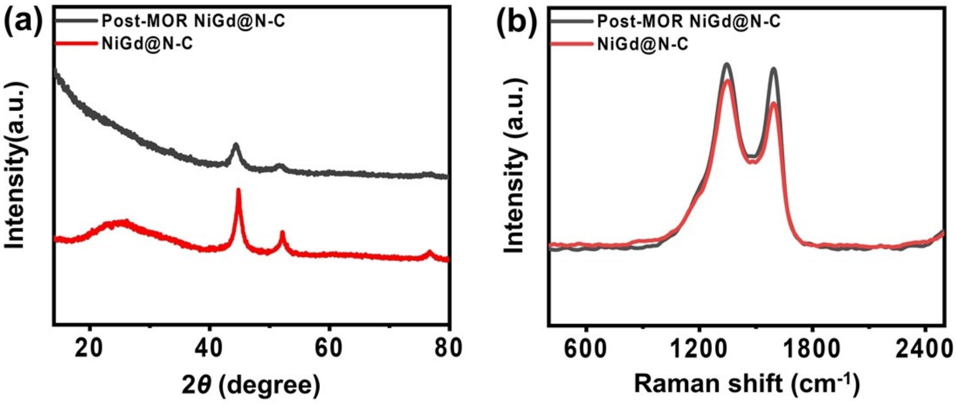

Fig. S14 XRD patterns and Raman spectra of the initial and post-MOR NiGd@N-C.

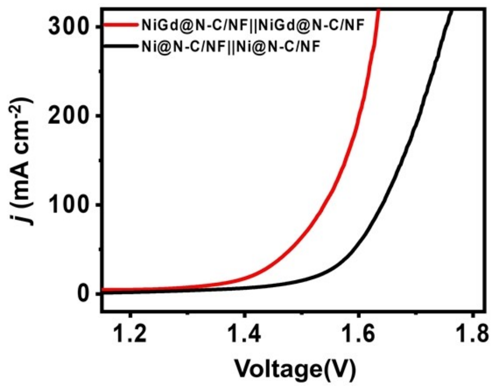

Fig. S15 LSV plots for NiGd@N-C/NF||NiGd@N-C/NF system and Ni@N-C/NF||Ni@N-C/NF in 1.0 M KOH solution with 3.0 M methanol.

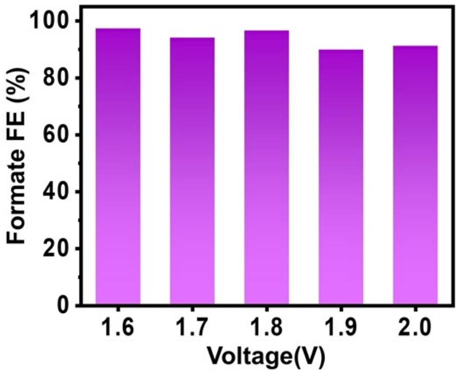

Fig. S16 The FEs of NiGd@N-C/NF||NiGd@N-C/NF system for formate production electrolysis at different cell voltages for 2 h.

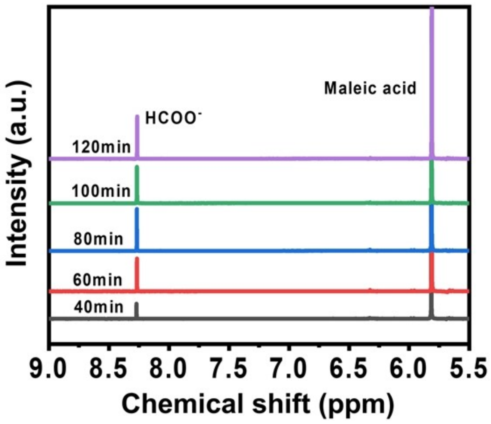

Fig. S17 The ^{1}H NMR results for the NiGd@N-C/NF||NiGd@N-C/NF system during different electrolysis times at 1.8 V. Maleic acid is used as an internal standard for the quantification of formate.

Table S1. Comparison of the chemical-assisted hydrogen evolution reaction performance for NiGd@N-C/NF and some other previously reported bifunctional catalysts.

Bifunctional catalysts	**Electrolyte**	**Main anode product**	**Cell voltage (V) 10 mA cm^{-2}**	**Ref.**
NiGd@N-C/NF	**1.0 M KOH+ 3.0 M methanol**	**formate**	**1.34**	**This work**
Ni(OH)$_2$/NF	1 M KOH + 0.5 M methanol	formate	1.52	8
Ir-Co$_3$O$_4$/NF	1.0 M KOH+ 0.1 M glycerol	formate	1.40	9
CoNi alloy	1 M KOH + 0.1 M glucose	gluconic acid	1.39	10
Co$_3$S$_4$-NSs/Ni-F	1 M KOH + 0.5 M ethanol	potassium acetate	1.48	11
Co-S-P/CC	1 M KOH + 1.0 M ethanol	acetic acid	1.63	12
Os-NixP/N-C/NF	1.0 M KOH+ 1.0 M methanol	formate	1.43	13
CoxP@NiCo-LDH/NF	1 M KOH + 0.5 M methanol	formate	1.43	14
Co$_{0.83}$Ni$_{0.17}$/AC	1.0 M KOH +10 mM benzyl alcohol	benzoic acid	1.43	15

References

1. J. Y. Wang, L. P. Sun, Q. Li, L. H. Huo and H. Zhao, Mater. Today Chem., 2023, 27, 101338.
2. Y. Xu, T. Liu, K. Shi, H. Yu, K. Deng, X. Wang, Z. Wang, L. Wang and H. Wang, J. Mater. Chem. A., 2022, 10, 20365-20374.
3. J. H. G. Kresse, Phys. Rev. B. , 1993, 48, 13115.
4. P. E. Blochl, Phys. Rev. B. Condens. Matter., 1994, 50, 17953-17979.
5. J. P. Perdew, J. A. Chevary, S. H. Vosko, K. A. Jackson, M. R. Pederson, D. J. Singh and C. Fiolhais, Phys. Rev. B. Condens. Matter., 1992, 46, 6671-6687.
6. T. B. J. K. Norskov, A. Logadottir, J. R. Kitchin, T. Bligaard,H. Jo´nsson, J. Phys. Chem. B., 2004, 108, 17886-17892.
7. C. Guo, X. Tian, X. Fu, G. Qin, J. Long, H. Li, H. Jing, Y. Zhou and J. Xiao, ACS Catal., 2022, 12, 6781-6793.
8. J. Hao, J. Liu, D. Wu, M. Chen, Y. Liang, Q. Wang, L. Wang, X.-Z. Fu and J.-L. Luo, Appl. Catal. B: Environ., 2021, 281, 119510.
9. Y. Xu, T. Liu, K. Shi, H. Yu, K. Deng, Z. Wang, X. Li, L. Wang and H. Wang, Chem Commun (Camb). 2023, 59, 1817-1820.
10. C. Lin, P. Zhang, S. Wang, Q. Zhou, B. Na, H. Li, J. Tian, Y. Zhang, C. Deng, L. Meng, J. Wu, C. Liu, J. Hu and L. Zhang, J. Alloys Compd., 2020, 823, 153784.
11. Y. Ding, Q. Xue, Q. L. Hong, F. M. Li, Y. C. Jiang, S. N. Li and Y. Chen, ACS. Appl. Mater. Inter., 2021, 13, 4026-4033.
12. S. Sheng, K. Ye, L. Sha, K. Zhu, Y. Gao, J. Yan, G. Wang and D. Cao, Inorg. Chem. Front., 2020, 7, 4498-4506.
13. Z. Duan, T. Ren, Q. Mao, H. Yu, K. Deng, Y. Xu, Z. Wang, L. Wang and H. Wang, J. Mater. Chem. A., 2022, 10, 18126-18131.
14. M. Li, X. Deng, Y. Liang, K. Xiang, D. Wu, B. Zhao, H. Yang, J.-L. Luo and X.-Z. Fu, J. Energy Chem., 2020, 50, 314-323.
15. G. Liu, X. Zhang, C. Zhao, Q. Xiong, W. Gong, G. Wang, Y. Zhang, H. Zhang and H. Zhao, New J. Chem., 2018, 42, 6381-6388.